Radiative Transfer in QSO Accretion Disk Winds: A First Year Report

James Matthews
Supervisor: Prof. Christian Knigge
School of Physics & Astronomy, University of Southampton, Southampton, SO17 1BJ, UK

31 July 2013

ABSTRACT
Broad Absorption Lines (BALs) are seen in $\sim 20\%$ of Quasi-Stellar Objects (QSOs) and are the most direct evidence of accretion disk winds in QSOs. I present here a first-year interim report on a project to learn about the true geometry of QSO winds informed by use of a Monte Carlo radiative transfer code. This code produces synthetic spectra for different viewing angles in a biconical disk wind model. In particular, the project focuses on two main areas; firstly, testing and improving the 'macro-atom' operation mode, so that line transfer can be treated without simplification, and secondly the question of QSO unification and whether a smooth, biconical wind model can produce broad emission lines in addition to BALs. In addition to presenting some preliminary results, I outline areas for future work and strategies for addressing the limitations of a current benchmark model.

1 INTRODUCTION

Outflows are crucial to our understanding of Active Galactic Nuclei (AGN) and Quasi-Stellar Objects (QSOs), due to their ubiquity (Ganguly & Brotherton 2008) and effect on spectral features at multiple wavelengths (e.g. Turner & Miller 2009, Weymann et al. 1991). These outflows can take the form of highly collimated radio jets (Belloni 2010), or less collimated, mass-loaded accretion disk winds (Murray et al. 1995). The kinetic luminosity associated with these outflows is often large enough to be energetically significant compared to the mass of galactic bulge. Thus, both types of outflows are often invoked as possible feedback mechanisms when considering the correlation between black hole mass and velocity dispersion in galaxies (Silk & Rees 1998; Häring & Rix 2004; Fabian 2012).

Blue-shifted Broad Absorption Lines (BALs) provide the most direct evidence of winds, and are observed in hot stars (Morton 1967), the ultraviolet spectra of Cataclysmic Variables (CVs; Greenstein & Oke 1982) and the subclass of QSO known as broad absorption line QSOs (BALQSOs). In addition, evidence of outflowing material can be seen in X-ray binaries (XRBs; Fender 2006; Ponti et al. 2012)

Here I present a report detailing work done during the first year of a PhD project. This project is broadly defined as an investigation into how radiative transfer can help improve our understanding of disk winds and outflows, with particular attention to testing unified QSO models.

1.1 BALQSOs

BALQSOs seem to be drawn from the same population as non-BAL QSOs (Reichard et al. 2003), and are believed to make up approximately 20% of the QSO population (Knigge et al. 2008), although the figure could be as high as $\sim 40\%$ (Allen et al. 2011). QSO unification models (e.g. Elvis 2000; Murray et al. 1995) propose that the intrinsic BALQSO fraction can be interpreted as the covering factor of an accretion disk wind. Some unification models also attempt to explain the Narrow Absorption Lines (NALs; Elvis 2000) and Broad Emission Lines (BELs; Veron-Cetty & Veron 2000) seen in QSOs. Due to their velocity spread, it is reasonable that BEL regions might be associated with the same disk wind

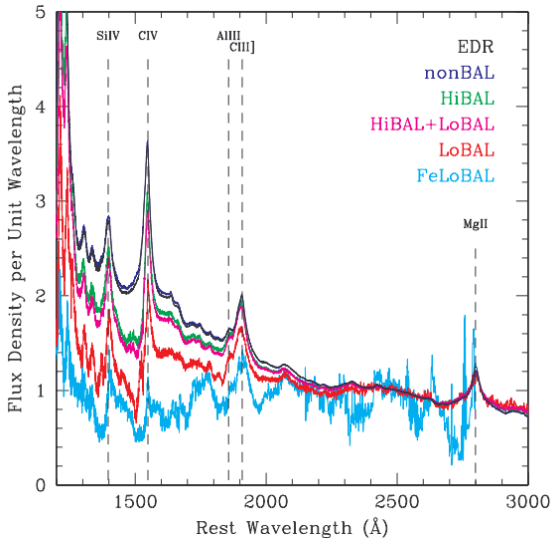

Figure 1. Normalized composite spectra for different types of BALQSOs compared to the full SDSS Early Data Release QSO sample (from Reichard et al. 2003)

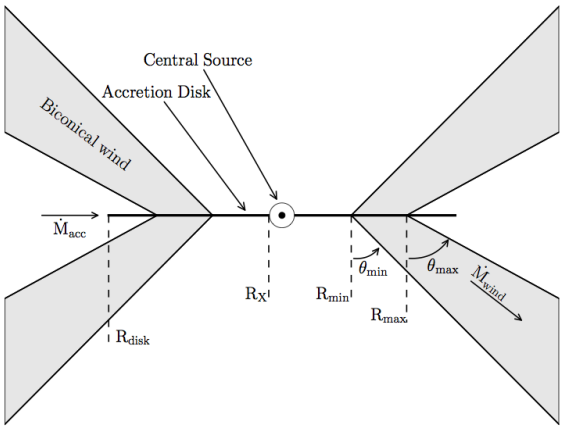

Figure 2. The geometry of the benchmark model desribed by H13. This is based on the Shlosman & Vitello (1993) prescription for CVs.

as BAL regions, although the extent to which they are co-spatial is not clear (Sulentic et al. 2000).

Figure 1 shows a comparison between different types of BALQSO and the full SDSS Early Data Release QSO sample (Reichard et al. 2003). BALQSOs with different levels of ionization can be seen in the figure, but all show blue-shifted absorption lines in high ionisation species such as as C IV , Si IV and N V. It is useful to define the ionization parameter,

$$\eta = \frac{N_{phot}}{4\pi r^2 n_H}, \quad (1)$$

at a given density, n_H, at a radius, r, from a source of N_{phot} ionizing photons. In AGN the central X-ray source causes an abundance of ionizing photons and a value for η which is overly large even for the highest-ionization BAL species. For this reason, a shielding region is often invoked as a way of attenuating the X-ray photons and controlling η to levels consistent with abundances of C IV , Si IV and N V (Murray et al. 1995; Gallagher & Everett 2007).

1.2 Disk Wind Models and Driving Mechanisms

Our team has embarked on a project to investigate different QSO geometries using a simple biconical wind geometry, shown in figure 2. The basic model involves a biconical wind which is launched from the accretion disk. The launching and driving mechanisms for disk winds are not yet properly understood, and, depending on the mass and type of system, some combination of thermal driving, line driving and magnetic driving (Blandford & Payne 1982) is thought to be responsible (see Proga 2007 for a review of potential driving mechanisms). With this uncertainty in mind, our model uses a flexible velocity law that can be adjusted with free parameters (see LK02) in attempts to reproduce observed results.

This model assumes, for the time being, that the wind is a smooth medium. However, 'clumpy' wind models, in which the outflowing materials in confined into clouds and clumps by magnetic forces have been suggested (e.g. De Kool & Begelman 1995; Emmering et al. 1991). We have considered an implementation similar to that described by Stalevski et al. (2013) as a way of controlling both the ionization parameter (e.g. Hamann et al. 2013) and emission of the wind. See §4 for more details.

2 MONTE CARLO RADIATIVE TRANSFER SIMULATIONS

It is difficult to build a coherent picture of the QSO population from observations alone. Fortunately, radiative transfer techniques are available which enable us to investigate certain disk wind models with Monte Carlo (MC) simulations. Many such simulations use the Sobolev aproximation, in which thermal broadening is assumed to be insignificant compared with the local velocity gradient (Hummer & Rybicki 1985). MC/Sobolev techniques have been applied to a variety of radiative transfer problems, such as Supernovae (Lucy 1999), CV disk winds (Knigge et al. 1995; Shlosman & Vitello 1993; Vitello & Shlosman 1993), Wolf-Rayet stars (Lucy & Abbott 1993) and AGN/QSO winds (Sim et al. 2008). Magneto-hydrodynamical (MHD) simulations with simpler radiative transfer implementations complement this work by providing insight into plausible driving mechanisms and realistic density profiles in AGN/QSO winds (Proga et al. 2000; Proga & Kallman 2004).

2.1 Python: A radiative transfer code

In addition to being the name of a widely used programming language, PYTHON (Long & Knigge 2002; hereafter LK02) is also the name of a MC/Sobolev radiative transfer code, written in C. It produces synthetic spectra for systems with outflowing material by tracking photons through a predefined system geometry, with adjustable size and discretisation. The simulations are carried in a 2-dimensional grid, which is applicable to 3 dimensions in geometries such as that shown in figure 2.

First, the temperature and ionization state of the wind is computed iteratively by passing photons through the wind and balancing heating and cooling processes. Second, photons are passed through a converged wind model and collected at user-specified inclination angles. This procedure is outlined in figure 3. PYTHON was originally used with CVs (LK02) but has also been applied to YSOs (Sim et al. 2005; S05) and, most recently, QSOs (Higginbottom et al. 2013; hereafter H13).

In its standard operating mode, PYTHON uses a two-level atom approximation (see e.g Mihalas 1982, Ch. 11) for its treatment of lines. This approximation works well when treating so-called 'resonance lines' (such as C IV , OVI), in which the excited electron is strongly coupled to the ground state, but breaks down for more complex situations such as recombination cascades. To properly model recombination lines, including the Lyman and Balmer series, a more complete treatment of line transfer is required.

2.2 Macro-Atoms

Lucy (2002, 2003; hereafter L02, L03) showed that by quantising matter into 'macro-atoms', and radiant and kinetic energy into energy packets, it is possible to asymptotically reproduce the emisssivity of a gas in statistical equilibrium

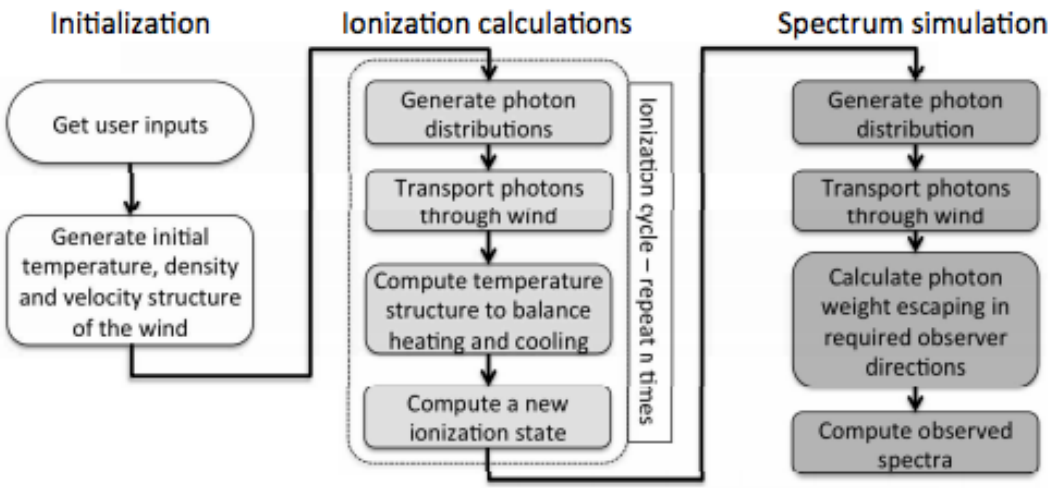

Figure 3. A schematic describing the procedure during a PYTHON run (from Higginbottom et al. 2012).

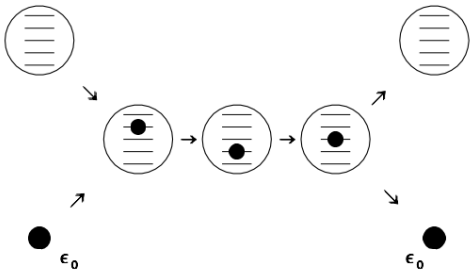

Figure 4. An energy packet of energy ϵ_0, activates a macro atom. The macro atom undergoes a series of internal transitions and then de-activates, emitting an energy packet. The energy of the emitted packet is rigidly conserved, but its frequency or type can change, e.g. from an r-packet to a k-packet (From Lucy 2002).

without simplifying line transfer. Macro-atoms are finite volume elements with internal transition probabilities that are 'activated' by packets of radiant (r-packets) or kinetic (k-packets) energy. A typical activation and deactivation sequence is shown in figure 4. A full description is far beyond the scope of this report- consult L02 and L03.

The macro-atom scheme has been used with PYTHON before, in a Hydrogen-only mode with application to YSOs (Sim et al. 2005), but has not yet been applied to AGN or CV problems. With some improvements, the current scheme will enable PYTHON to model H and He recombination lines, for example. The fast, simple treatment of resonance lines can be retained, as the PYTHON implementation allows for non-macro atom treatment for certain ions.

3 INITIAL RESULTS AND DISCUSSION

H13 present a benchmark disk wind model which successfully reproduces some aspects of BALQSO spectra (see figure 5). However, inspection of the model reveals three key shortcomings. First, the X-ray luminosity of the system is weak. The unattenuated luminosity is already low for a BALQSO, and should be comparable to a non-BAL QSO if a unified disk wind model is capable of explaining BALs. In addition, X-rays are attenuated by the disk wind and mean that for BAL angles the luminosity observed is low for a BALQSO. Second, the model fails to reproduce BELs, as not enough thermal line emission is produced. Third, the fiducial model fails to correctly model the Ly-α line, for the reasons outlined in §2.1. Fortunately, some progress has been made in addressing these three problems.

3.1 Thermal Line Emission

It has been proposed that thermal line emission- radiation produced by the relaxation of collisionally excited bound electrons to lower energy states within the ion- is the dominant mechanism responsible for the BELs we see in QSOs (Murray et al. 1995), although this is by no means a consensus[1] When considering collisionally exited line emission, it is useful to define the emission measure, Y, of a plasma of volume V (Kaastra et al. 2008)

$$Y = \int_0^V n_e n_H \, dV \tag{2}$$

Note that this emission measure is defined in terms of Hydrogen. The strength of a collisionally-excited emission line will thus depend on the density and scale of the wind, and the relative abundance of the ion responsible for the line in question. The velocity law and opening angle of the wind will also have a profound impact, as they allow for variation not only of how dense the medium is, but also *where* it is dense and what the ionization state is at a given point. Figure 6 shows an example of a model which is designed to

[1] By way of example, Krolik & Voight (1998) find a covering angle of ~ 0.5 for absorbing material in BALQSOs by considering inherent bias against BALQSO discovery in optical flux-limited samples. This greater covering factor would mean that scattered radiation could have a more important role.

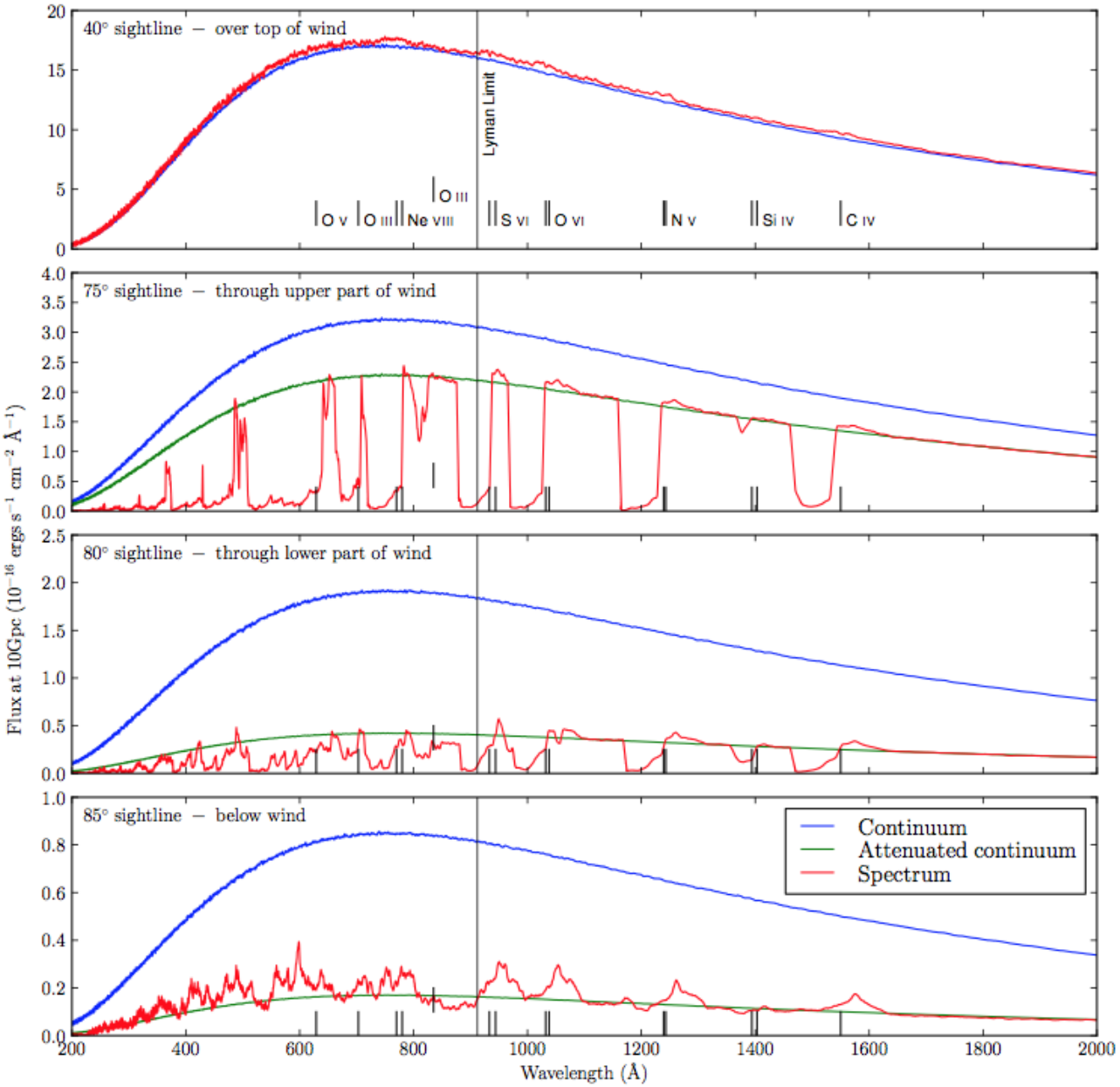

Figure 5. Benchmark model spectra for four sightlines from H13. In this model, θ_{min} and θ_{max} (defined in figure 2) are 70° and 82° respectively

Table 1. A comparison of the benchmark model from H13 (Model A) and a model designed to produce increased thermal line emission (Model B). The output spectra are presented in figure 6.

Parameter	Model A	Model B
$\dot{M}_{wind}(M_\odot/yr)$	5	25
α	1	4

produce more thermal line emission. The properties of the model are summarised in table 1.

An exploration of the parameter space and different geometries is required (see §4), as this model fails to reproduce BALs in the all the required lines for angles looking through the wind. However, it demonstrates that a modest alteration to the H13 benchmark model can cause a dramatic increase in collisionally-excited line strength.

3.2 X-ray properties

The problematic weak X-ray flux in the benchmark model is somewhat related to the weak line emission in the model. This is because the ionization parameter of a plasma, η, depends on both the intensity of the X-ray flux and the density

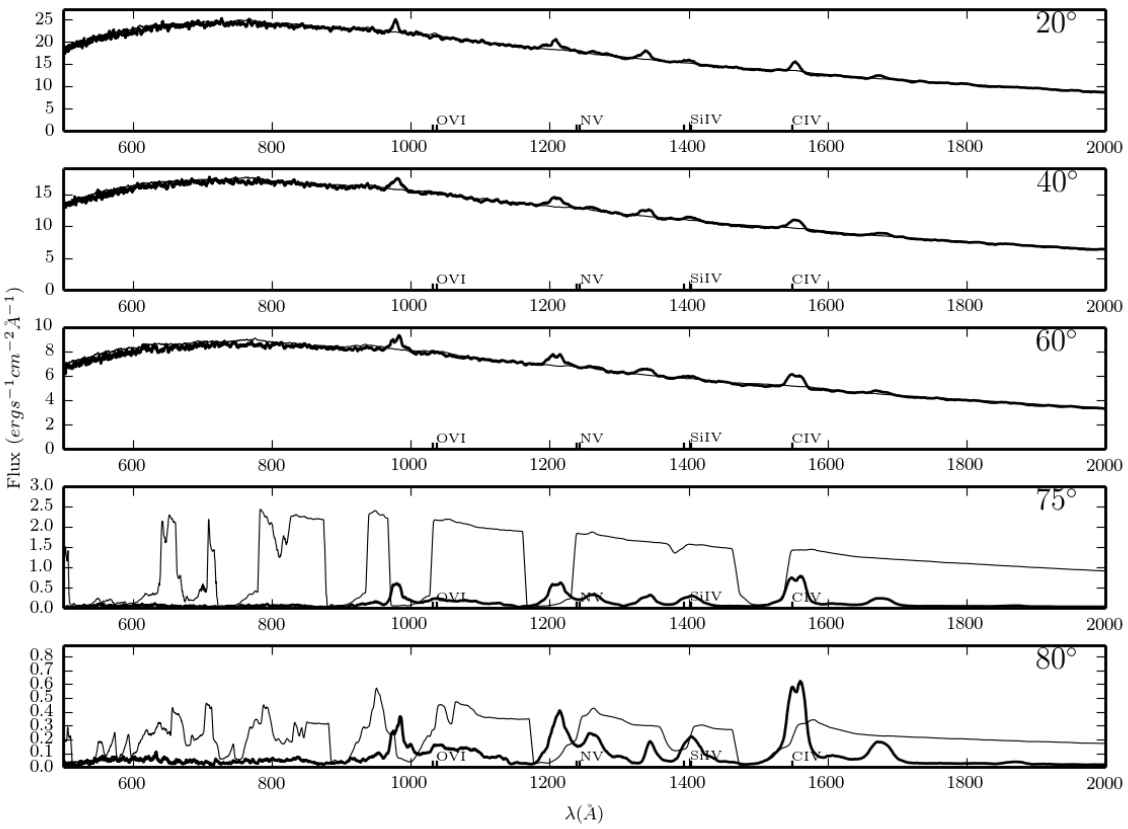

Figure 6. A comparison of PYTHON spectra outputs for Model A (thin line) Model B (thick line). Different sightlines to H13 are shown to illustrate the line emission at low inclinations.

of the plasma. Thus, changing the model to increase density in certain parts of the wind (by careful tweaking of the wind parameters, mass loss rate and $2-10$ KeV luminosity) can lead to a twofold improvement, as the emission measure and X-ray luminosity can potentially be increased while preserving the required ionization parameter to produce BALQSO UV resonance lines.

In addition, the accuracy of the X-ray treatment in PYTHON is limited by atomic data. Currently, PYTHON uses The Opacity Project online database (`TOPbase`; Badnell et al. 2005) for photoionization cross-sections. Unfortunately, the cross sections have maximum energies associated with them, and in our model we see an artifical 'edge' in the X-ray spectra due to the OV data (see figure 7). OV has a maximum energy of 4081 eV and has significant photoionization opacities through the wind, which causes the problem. To improve on this, we plan on exploring other sources of atomic data such as AtomDB (Foster et al. 2012). Figure 7 also shows X-ray data produced using the `standard_extrap` data set (our extrapolated version of `TOPbase` data). The sharp edge diappears, and a smooth recovery to the X-ray power law is observed.

The change in X-ray SED does not affect the UV spectra or ionization state of the wind in the benchmark model, due to the X-ray weakness. However, if we hope to present a model with more realistic X-ray properties then a robust treatment of photoionization cross-sections at high energies is essential.

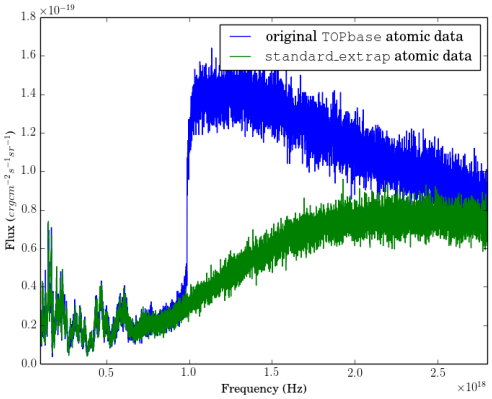

Figure 7. X-ray spectra of the H13 benchmark model with original `TOPbase` data, compared against the extrapolated `TOPbase` data set, `standard_extrap`. This spectrum is for an observer inclination of 85° (Close to edge-on).

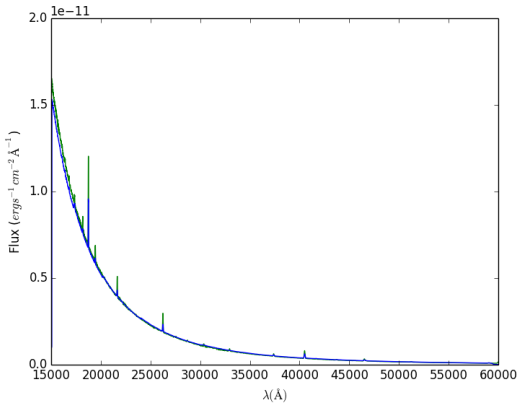

Figure 8. A YSO model comparison between PYTHON 76 (green) and S05. The line emission is substantially higher in PYTHON 76.

3.3 Macro Atoms in Python

I have conducted tests of the macro atom mode in PYTHON with YSO models. At the time of writing, this has revealed that the latest version of the code, PYTHON 76, does not agree with the models described by S05, as shown in figure 8. The line strengths of the Brackett and Paschen hydrogen lines are different, with the latest version of PYTHON producing much more line emission from the base of the wind. The reason for this is as yet unclear, but test codes are currently being devised to isolate the problem.

4 SUMMARY & FUTURE WORK

I plan on focusing future work in a number of key areas.

4.1 Macro Atoms

A priority for producing realistic recombination line profiles is to continue testing and developing the macro atom scheme in PYTHON . This will involve encorporating He atomic data and attempting to reproduce He recombination lines in CVs and Ly-α emission in BALQSO spectra. Once the YSO models shown in figure 8 have been verified, tests involving simple toy models and comparisons against CLOUDY (Ferland et al. 2013) can be carried out to check the implementation.

4.2 Improving the Benchmark Model

The benchmark model of H13 can be improved by altering the model such that it has a realistic X-ray flux and so it can reproduce the observed BELs in QSOs. This will involve an extended investigation of a number of parameters; the velocity law of the wind, the opening angle of the wind, the launch radius, the X-ray luminosity and the mass loss rate through the wind, $\dot{M}_W$.

4.3 Wider Context

The wider aim of this project is to test how many, if any, of the spectral features seen in QSOs can be explained by a smooth biconical disk wind. Success will depend on whether a better attempt at a unified QSO model can be produced. If this is not possible, it may be necessary to consider additions to our simple model. This may include, but is not limited to, altering the geometry of the model, modifying the velocity law of the wind and including clumping in the flow.

Throughout this process, we will consider the implications for AGN feedback, and depending on progress we may be able to draw conclusions as to the level of feedback a smooth, biconical wind can be responsible for. The key quantity when considering feedback implications is the kinetic luminosity, $\dot{E}_K = 1/2\dot{M}_W v^2$. $\dot{M}_W$ is an important quantity which can alter observed features significantly, and so cannot be purely motivated by feedback considerations.

ACKNOWLEDGEMENTS

I would like to thank the PYTHON team for their invaluable help and for use of the code: Knox Long, Christian Knigge, Nick Higginbottom and Stuart Sim. In addition I would like to thank Christian Knigge for supervising this work. This document was prepared using the `mn2e` LATEX macros, and simulation outputs are from PYTHON 76. This work is supported by the Science and Technology Facilities Council (STFC).

REFERENCES

Allen J. T., Hewett P. C., Maddox N., Richards G. T., Belokurov V., 2011, MNRAS 410, 860
Badnell N. R., Bautista M. A., Butler K., Delahaye F., Mendoza C., Palmeri P., Zeippen C. J., Seaton M. J., 2005, MNRAS 360, 458
Belloni T. (ed.), 2010, The Jet Paradigm, Vol. 794 of *Lecture Notes in Physics, Berlin Springer Verlag*
Blandford R. D., Payne D. G., 1982, MNRAS 199, 883
de Kool M., Begelman M. C., 1995, ApJ 455, 448
Elvis M., 2000, ApJ 545, 63
Fabian A. C., 2012, ARAA 50, 455
Fender R., 2006, Jets from X-ray binaries, 381–419
Ferland G. J., Porter R. L., van Hoof P. A. M., Williams R. J. R., Abel N. P., Lykins M. L., Shaw G., Henney W. J., Stancil P. C., 2013, RMXAA 49, 137
Foster A. R., Ji L., Smith R. K., Brickhouse N. S., 2012, The Astrophysical Journal 756(2), 128
Gallagher S. C., Everett J. E., 2007, in L. C. Ho, J.-W. Wang (eds.), The Central Engine of Active Galactic Nuclei, Vol. 373 of *Astronomical Society of the Pacific Conference Series*, 305
Ganguly R., Brotherton M. S., 2008, ApJ 672, 102
Greenstein J. L., Oke J. B., 1982, ApJ 258, 209
Hamann F., Chartas G., McGraw S., Rodriguez Hidalgo P., Shields J., Capellupo D., Charlton J., Eracleous M., 2013, ArXiv e-prints
Häring N., Rix H.-W., 2004, ApJ Letters 604, L89
Higginbottom N., Long K. S., Knigge C., Sim S. A., 2012, in G. Chartas, F. Hamann, K. M. Leighly (eds.), AGN Winds in Charleston, Vol. 460 of *Astronomical Society of the Pacific Conference Series*, 194
Higginbottom N. S., Knigge C., Long K. S., Sim S. A., Matthews J. H., 2013, Submitted to MNRAS

Hummer D. G., Rybicki G. B., 1985, ApJ 293, 258
Kaastra J. S., Paerels F. B. S., Durret F., Schindler S., Richter P., 2008, SSR 134, 155
Knigge C., Scaringi S., Goad M. R., Cottis C. E., 2008, MNRAS 386, 1426
Knigge C., Woods J. A., Drew J. E., 1995, MNRAS 273, 225
Krolik J. H., Voit G. M., 1998, ApJ Letters 497, L5
Long K. S., Knigge C., 2002, ApJ 579, 725
Lucy L. B., 1999, A&A 345, 211
Lucy L. B., 2002, A&A 384, 725
Lucy L. B., 2003, A&A 403, 261
Lucy L. B., Abbott D. C., 1993, ApJ 405, 738
Mihalas D. M., 1982, Stellar atmospheres.
Morton D. C., 1967, ApJ 150, 535
Murray N., Chiang J., Grossman S. A., Voit G. M., 1995, ApJ 451, 498
Ponti G., Fender R. P., Begelman M. C., Dunn R. J. H., Neilsen J., Coriat M., 2012, MNRAS 422, L11
Proga D., 2007, in L. C. Ho, J.-W. Wang (eds.), The Central Engine of Active Galactic Nuclei, Vol. 373 of *Astronomical Society of the Pacific Conference Series*, 267
Proga D., Kallman T. R., 2004, ApJ 616, 688
Proga D., Stone J. M., Kallman T. R., 2000, ApJ 543, 686
Reichard T. A., Richards G. T., Hall P. B., Schneider D. P., Vanden Berk D. E., Fan X., York D. G., Knapp G. R., Brinkmann J., 2003, AJ 126, 2594
Shlosman I., Vitello P., 1993, ApJ 409, 372
Silk J., Rees M. J., 1998, A&A 331, L1
Sim S. A., Drew J. E., Long K. S., 2005, MNRAS 363, 615
Sim S. A., Long K. S., Miller L., Turner T. J., 2008, MNRAS 388, 611
Stalevski M., Fritz J., Baes M., Popovic L. C., 2013, ArXiv e-prints
Sulentic J. W., Marziani P., Dultzin-Hacyan D., 2000, ARAA 38, 521
Turner T. J., Miller L., 2009, AAPR 17, 47
Véron-Cetty M. P., Véron P., 2000, AAPR 10, 81
Vitello P., Shlosman I., 1993, ApJ 410, 815
Weymann R. J., Morris S. L., Foltz C. B., Hewett P. C., 1991, ApJ 373, 23